A Practical Approach to Landmark Deployment for Indoor Localization

Yingying Chen, John-Austen Francisco, Wade Trappe, Richard P. Martin
{yingche,deymious,rmartin}@cs.rutgers.edu, trappe@winlab.rutgers.edu
Department of Computer Science and Wireless Information Network Laboratory
Rutgers University, 110 Frelinghuysen Rd, Piscataway, NJ 08854

***Abstract*— We investigate the impact of landmark placement on localization performance using a combination of analytic and experimental analysis. For our analysis, we have derived an upper bound for the localization error of the linear least squares algorithm. This bound reflects the placement of landmarks as well as measurement errors at the landmarks. We next develop a novel algorithm, $maxL-minE$, that using our analysis, finds a pattern for landmark placement that minimizes the maximum localization error. To show our results are applicable to a variety of localization algorithms, we then conducted a series of localization experiments using both an 802.11 (WiFi) network as well as an 802.15.4 (ZigBee) network in a real building environment. We use both Received Signal Strength (RSS) and Time-of-Arrival (ToA) as ranging modalities. Our experimental results show that our landmark placement algorithm is generic because the resulting placements improve localization performance across a diverse set of algorithms, networks, and ranging modalities.**

I. Introduction

Localization of nodes in wireless and sensor networks is important because the location of sensors is a critical input to many higher-level networking tasks, such as tracking, monitoring and geometric-based routing. Although recent efforts have resulted in a plethora of methods to localize sensor nodes, little work to date has systematically investigated how the placement of the nodes with known locations, or *landmarks*, impacts localization performance. In this work we investigate the impact of landmark placement on localization performance using a combination of analytic and experimental analysis.

Our analytic approach focuses on the Least Squares (LS) algorithm, and in particular, a variant we call Linear Least Squares (LLS). Our analysis centers on the algorithm for two reasons. First, LS is a widely used multilateration algorithm, as is evidenced by its application as a step in many recent localization research works [1]–[5]. Second, mathematical analysis of LLS is tractable, resulting in equations with closed-form solutions. For a myriad of other algorithms, closed form solutions that describe the localization error as a function of landmark placement are not tractable and as a result heuristic search strategies must be used to find an optimal placement, as was done in [6].

Our analysis of landmark placement can find an optimal placement of landmarks in well-defined regular regions, thus making it quite suitable for indoor localization. The analysis begins with LLS and places an upper bound of the maximum localization error given a set of landmark placements. We can show that this upper bound is minimized by a combination of minimizing the distance estimation error together with the employment of the optimal patterns for landmark placement.

Using this result, we can compare the maximum error between any two placements. We can then constrain a search of placements to minimize the maximum error. We have developed a simple algorithm called $maxL - minE$ algorithm that finds an optimized landmark deployment for the LLS algorithm.

We show that our placement minimizing the upper bounds of LLS also reduces the Hölder parameter for a variety of algorithms. The Hölder parameter [7] describes the maximum change in physical space that can arise from a change in signal space. This is strong evidence that our $maxL - minE$ algorithm finds a landmark placement that minimizes the errors due to noise, bias, and measurement error.

Another interesting result of our analysis is that for a small number of landmarks, simple shapes such as equilateral triangles and squares result in placements with better localization performance. Interestingly, for higher number of landmarks, we can show that extensions of shapes with equal sides, e.g. a hexagon, are non-optimal. Rather, the simple shapes enclose one another, for example, two enclosing equilateral triangles. We detail these geometries and describe rule-of-thumb for landmark placement in Section III.

To show the generality of our results, we conducted localization experiments with both an 802.11 (WiFi) network as well as an 802.15.4 (ZigBee) network in a real building environment. For the 802.11 network,

we used two ranging modalities, Received Signal Strength (RSS) to distance, and Time of Arrival (TOA). In the 802.15.4 network, we used only RSS-to-distance.

We compared the accuracy of a suite of localization algorithms using landmarks placed according to our analysis as well as landmarks placed in positions that provide good signal coverage but ignore localization concerns. While we found that all algorithms improved their performance, over a non-optimal placement for localization, we also observed that LS became competitive with the other algorithms, and that coarse-grained TOA ranging was less accurate than RSS-based approaches.

The remainder of the paper is as follows. Section II discusses previous research in localization. We provide the theoretical analysis in Section III. Then Section IV describes the metrics that we use to characterize the localization performance. The investigation of the number of landmarks and their positions is provided in Section V. Section VI presents the experimental results across localization algorithms, networks, and ranging strategies. Finally we bring our conclusion in Section VII.

II. Related Work

There have been many active research efforts developing localization systems for wireless and sensor networks. We cannot cover the entire body of works in this section. Rather, we give a short overview of the different localization strategies and then describe the works most closely related to ours.

The localization techniques can be categorized along several dimensions. Range-based algorithms involve distance estimation to landmarks using the measurement of various physical properties [8] like RSS [9], [10], Time Of Arrival (TOA) [1] and Time Difference Of Arrival (TDOA) [11]. While range-free algorithms [2], [12] use coarser metrics to place bounds on candidate positions. Another method of classification describes the strategy used to map a node to a location. Lateration approaches [1]–[5], use distances to landmarks, while angulation uses the angles from landmarks. Scene matching strategies [9], [10], [13], [14] use a function that maps observed radio properties to locations on a pre-constructed radio map or database. Scene matching is often used in indoor environments because local conditions distort the signal propagation from free space models. Finally, a third dimension of classification extends to aggregate [12], [15] or singular algorithms.

Our work is novel in that instead of improving the localization algorithms themselves, we focus on improving the deployment of landmarks, and this should help a wide variety of algorithms.

[16] used simple linear and multiple regression methods to estimate the signal strength model. With simulation, it analyzed the relationship between standard deviation of location error and signal strength error for a few Access Point (AP) configurations. However, They did not analyze for the optimized geometry of AP deployment and provide experimental comparison as we have in our work. Another work examined placement, but did not find optimal solutions [17]. [6] developed a set of heuristic search algorithms to find optimal AP deployment for a balance of signal coverage and location errors. Compared to our simple approach, the heuristic search algorithms are more complex and time consuming. The results were only shown for the probability matching algorithms, thus may not be general for other type of algorithms.

Finally, a large body of works have examined AP placement to maximize coverage and throughput properties of Wireless LANs and sensor networks. We do not cover these works here, except to say that future work would be to examine the tradeoffs in landmark and AP deployment assuming they use the same hardware, although this does not need to be the case. Recall that landmarks provide a node with signals from known locations, while APs provide media access control as well as gateways into the wired network.

III. Theoretical Analysis

In this section we first provide background on using LS algorithms for localization, and then describe the LLS variant. We next present our theoretical analysis of an upper bound on the error, and then discuss our $maxL - minE$ placement algorithm.

A. Background: Localization with LS

To perform localization with LS requires 2 steps: ranging and lateration.

Ranging Step: Recent research has seen a host of variants on the ranging step. For example, in the APS algorithm [2], hop counts are used to estimate ranges. Other approaches are also possible, [11] used the time-difference of arrival between an ultrasound pulse and a radio packet. In this work, we focus on RSS and TOA as ranging strategies.

Lateration Step: From the estimated distances d_i and known positions (x_i, y_i) of the landmarks, the position (x, y) of the localizing node can be found by finding $(\hat{x}, \hat{y})$ satisfying:

$$(\hat{x}, \hat{y}) = arg\min_{x,y} \sum_{i=1}^{N} [\sqrt{(x_i - x)^2 + (y_i - y)^2} - d_i]^2 \quad (1)$$

where N is the total number of landmarks. We call solving the above problem *Nonlinear Least Squares*, or NLS. It can be viewed as an optimization problem where the objective is to minimize the sum of the error square.

Solving the NLS problem requires significant complexity and is difficult to analyze. We may approximate the NLS solution and linearize the problem by introducing a constraint in the formulation. We start with the $N \geq 2$ equations:

$$\begin{aligned} (x_1 - x)^2 + (y_1 - y)^2 &= d_1^2 \\ (x_2 - x)^2 + (y_2 - y)^2 &= d_2^2 \\ &\vdots \\ (x_N - x)^2 + (y_N - y)^2 &= d_N^2 \end{aligned} \tag{2}$$

Now, subtracting the constraint

$$\frac{1}{N}\sum_{i=1}^{N}[(x_i - x)^2 + (y_i - y)^2] = \frac{1}{N}\sum_{i=1}^{N} d_i^2 \tag{3}$$

from both sides, we obtain the following set of linear equations

$$\begin{aligned} &(x_1 - \frac{1}{N}\sum_{i=1}^{N} x_i)x + (y_1 - \frac{1}{N}\sum_{i=1}^{N} y_i)y = \\ &\frac{1}{2}[(x_1^2 - \frac{1}{N}\sum_{i=1}^{N} x_i^2) + (y_1^2 - \frac{1}{N}\sum_{i=1}^{N} y_i^2) - (d_1^2 - \frac{1}{N}\sum_{i=1}^{N} d_i^2)] \\ &\vdots \\ &(x_N - \frac{1}{N}\sum_{i=1}^{N} x_i)x + (y_N - \frac{1}{N}\sum_{i=1}^{N} y_i)y = \\ &\frac{1}{2}[(x_N^2 - \frac{1}{N}\sum_{i=1}^{N} x_i^2) + (y_N^2 - \frac{1}{N}\sum_{i=1}^{N} y_i^2) - (d_N^2 - \frac{1}{N}\sum_{i=1}^{N} d_i^2)]. \end{aligned} \tag{4}$$

The above can be easily solved linearly using the form $\mathbf{Ax} = \mathbf{b}$ with:

$$\mathbf{A} = \begin{pmatrix} x_1 - \frac{1}{N}\sum_{i=1}^{N} x_i & y_1 - \frac{1}{N}\sum_{i=1}^{N} y_i \\ \vdots & \vdots \\ x_N - \frac{1}{N}\sum_{i=1}^{N} x_i & y_N - \frac{1}{N}\sum_{i=1}^{N} y_i \end{pmatrix} \tag{5}$$

and

$$\mathbf{b} = \frac{1}{2}\begin{pmatrix} (x_1^2 - \frac{1}{N}\sum_{i=1}^{N} x_i^2) + (y_1^2 - \frac{1}{N}\sum_{i=1}^{N} y_i^2) \\ -(d_1^2 - \frac{1}{N}\sum_{i=1}^{N} d_i^2) \\ \vdots \\ (x_N^2 - \frac{1}{N}\sum_{i=1}^{N} x_i^2) + (y_N^2 - \frac{1}{N}\sum_{i=1}^{N} y_i^2) \\ -(d_N^2 - \frac{1}{N}\sum_{i=1}^{N} d_i^2) \end{pmatrix}. \tag{6}$$

Note that $\mathbf{A}$ is described by the coordinates of landmarks only, while $\mathbf{b}$ is represented by the distances to the landmarks together with the coordinates of landmarks. We call the above formulation of the problem *Linear Least Squares*, or LLS. NLS trades higher computational complexity for better accuracy. The introduction of the constraint collapsed the nonlinear problem into a linear problem, which greatly simplifies the computation needed to arrive at a location estimate. In addition to its computational advantages, the LLS formulation allows for tractable error analysis, as we shall soon provide.

B. Error Analysis

Our objective is to minimize the location estimation error introduced by LLS. we have matrix $\mathbf{A}$ and vector $\mathbf{b}$ presented in Equations (5) and (6). In an ideal situation solving for $\mathbf{x} = [x, y]^T$ is done via

$$\mathbf{x} = (\mathbf{A}^T\mathbf{A})^{-1}\mathbf{A}^T\mathbf{b} \tag{7}$$

However, the estimated distances are impacted by noise, bias, and measurement error. We express the resulting distance estimation error $\mathbf{e}$ in terms of $\tilde{\mathbf{b}}$ with estimated distances and $\mathbf{b}$ with true distances as $\tilde{\mathbf{b}} = \mathbf{b} + \mathbf{e}$, and hence the localization result is

$$\tilde{\mathbf{x}} = (\mathbf{A}^T\mathbf{A})^{-1}\mathbf{A}^T\tilde{\mathbf{b}}. \tag{8}$$

The location estimation error is thus bounded by

$$\|\mathbf{x} - \tilde{\mathbf{x}}\| \leq \|\mathbf{A}^+\|\|\mathbf{e}\|, \tag{9}$$

where the matrix $\mathbf{A}^+$ is the Moore-Penrose pseudo-inverse of $\mathbf{A}$. It can be shown that, under the 2-norm, $\|\mathbf{A}^+\| = \frac{1}{\gamma_2}$, where $\gamma_1 \geq \gamma_2$ are the singular values of $\mathbf{A}$. This means that for a certain size on error $\mathbf{e}$ the LS estimation error is stretched by $\frac{1}{\gamma_2}$. It can be proved that the eigenvalues of $\mathbf{A}^T\mathbf{A}$ are the squares of the singular values of $\mathbf{A}$. Therefore, we can limit our concern to the eigenvalues of $\mathbf{A}^T\mathbf{A}$, where $\mathbf{A}^T\mathbf{A}$ is a matrix of the form:

$$\mathbf{A}^T\mathbf{A} = 4\begin{pmatrix} a & b \\ b & c \end{pmatrix}$$

with:

$$a = \sum_{i=1}^{N}(x_i - \frac{1}{N}\sum_{i=1}^{N} x_i)^2 \tag{10}$$

$$b = \sum_{i=1}^{N}[(x_i - \frac{1}{N}\sum_{i=1}^{N} x_i)(y_i - \frac{1}{N}\sum_{i=1}^{N} y_i)] \tag{11}$$

$$c = \sum_{i=1}^{N}(y_i - \frac{1}{N}\sum_{i=1}^{N} y_i)^2. \tag{12}$$

Note that a, b and c are only related to the coordinates of landmarks (x_i, y_i). The eigenvalues of $\mathbf{A}^T\mathbf{A}$ can be found as the roots of:

$$\lambda^2 - 4(a + c)\lambda + 16(ac - b^2) = 0.$$

Thus, we have:

$$\lambda = 4(a + c) \pm 2\sqrt{(a - c)^2 + 4b^2}, \tag{13}$$

where the discriminant, $(a-c)^2+4b^2$, is non-negative.

C. Deployment Patterns

Our goal in this section is to minimize the total error. Recall there are two terms on the right side of Equation (9). Our approach is to choose x_i and y_i so as to make λ_2 (the smaller eigenvalue) as close to λ_1 as possible, because this will minimize the first term, $\|\mathbf{A}^+\|$. Given the first term is minimized, we then minimize the second term. Having minimized the second term given the first term is minimized is clearly a local minima. We call such a local minima *an optimal deployment*, because no movement of a single landmark can improve the error bound. However, our piecewise minimization approach still leaves open a proof that this local minima is the true minima over all possible landmark positions. We leave such a proof as future work.

Returning to minimizing the first term $\|\mathbf{A}^+\|$, to minimize $\frac{1}{\sqrt{\lambda_2}}$, a general strategy would be to make $(a-c)$ small or to make b small or both. Interestingly, this is determined only by the coordinates of the landmarks.

Then our next task is to find the landmark positions that satisfy $\lambda_1 \cong \lambda_2$. We found that the optimal landmark deployment setup follows some simple and symmetric patterns. This makes it not only possible to achieve but also easy to deploy practically. Figure 1 shows the patterns for an optimal landmark deployment setup when utilizing 3, 4, 5, 6, 7, 8 landmarks in the indoor environment. These patterns consist of squares, equilateral triangles, or the enclosing of them. We observe that for higher number of landmarks, the extensions of shapes with equal sides, e.g. a hexagon, do not satisfy $\lambda_1 \cong \lambda_2$, and thus are not optimal. Instead, the simple shapes enclose one another present optimal solutions.

D. Finding an Optimized landmark Deployment

The above discussion dealt with deploying the landmarks without considering the physical constraints of the building and, as such, only provide a general guideline as to the "shape" of the deployment. Placing the landmarks within a particular building requires stretching/shrinking the deployment shape so that it fits within the confines of the building. The stretching/shrinking should be done so as to minimize localization errors.

Recall in Equation (9), the location estimation error is also contributed by $\|\mathbf{e}\|$, and that $\tilde{\mathbf{b}} = \mathbf{b} + \mathbf{e}$. The term $\|\mathbf{e}\|$ is a result of distance estimation errors introduced by ranging. We have developed an iterative algorithm, called $maxL - minE$ (i.e. maximum lambda and minimum error), which helps to find the real landmark coordinates given the floor

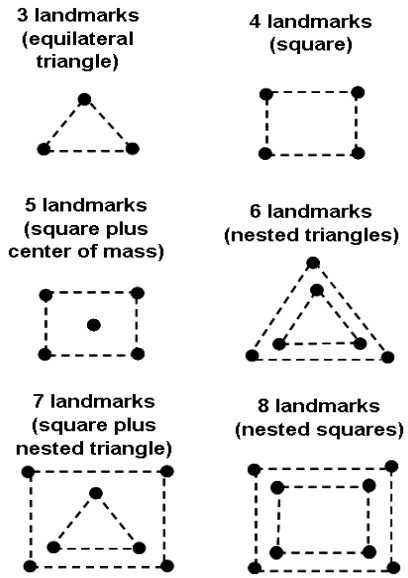

Fig. 1. Patterns for optimal landmark deployments

---

input $floorSize, numOfLandmark$
output $optimized\ \ landmark\ \ coordinates$

[initialize] get optimal pattern based on geometry
fit optimal pattern into maximum floorsize
generate initial landmark coordinates
calculate λ_1 and λ_2

$minError = maxNum$
loop until $thisError > minError$
  generate random localizing nodes
  for each localizing node **begin**
    apply random noise or bias
    $B = \|b - \tilde{b}\|$
  end for
  $thisError = \frac{avg(B)}{\sqrt{lambda_2}}$
  if $thisError < minError$, $minError = thisError$
  [landmark adjustment] move towards the center of mass one step
end loop
return $optimized\ \ landmark\ \ coordinates$

Fig. 2. The maxL-minE algorithm

size, number of landmarks, and the optimal landmark deployment pattern. Figure 2 shows the pseudo-code that implements $maxL - minE$. The algorithm first minimizes $\|\mathbf{A}^+\|$ using geometry, then uses an iterative search. The search begins with a maximal sized optimal pattern (e.g. a square) and simply keeps reducing the size of the pattern until such movements stop reducing the distance estimation error $\mathbf{e}$. We observe the algorithm usually converges very quickly within a number of iterations.

IV. Evaluation Metrics

In this section we describe the three metrics we use throughout the rest of the paper.

Average error: All of our observations are the results of many localization trials. This metric takes the average of the distances between the localized result and the true location over all trials. In area-based algorithms, as opposed to point-based ones, the result is a returned area. To compare these two kinds of algorithms, we use the median X and Y of the returned area to the true location to generate a point and then average these distance errors.

Accuracy CDF: We also return the entire cumulative density function (CDF) of all our localization attempts. We simply report all attempts in sorted order, and then normalize the Y axis by the total number of attempts to obtain a domain of $[0, 1]$. For area-based algorithms, we also report CDFs of the minimum and maximum error. For a given attempt, these are points in the returned area that are closest to and furthest from the true location.

Hölder Metrics: In addition to error performance, we are also interested in how dramatically the localization results can be perturbed by changes in signal strength. Hölder metrics for RSS based localization were introduced in a previous work [7]. Intuitively, these metrics relate the magnitude of a perturbation to its effect on the localization result. The idea here is that certain landmark placements can reduce the impacts of perturbations due to noise or bias, and we should be able to observe these as lower Hölder parameters.

The Hölder parameter H^p_{alg} for a given placement and algorithm is defined as $H^p_{alg} = \max_{\mathbf{s},\mathbf{v}} \frac{\|L^p_{alg}(\mathbf{s}) - L^p_{alg}(\mathbf{v})\|}{\|\mathbf{s}-\mathbf{v}\|}$, where L^p_{alg} is the result of a localization algorithm alg given placement p, with s as a signal strength vector and v as a perturbed vector.

Since the traditional Hölder parameter describes the maximum effect a perturbation might have, it is natural to also provide an average-case measurement. We therefore examine the average-case Hölder parameter, $\overline{H}^p_{alg}$, as well. In both cases, we measure the metrics by statistical sampling in the case of simulation, or direct computation over all localization attempts for experimentally measured data.

V. Landmark Position and Quantity

In this section we investigate the impact of landmark position and quantity on localization performance. Because the data collection process using many real deployments is prohibitively time-consuming, we use a trace-driven simulation methodology for this section. We first describe our methodology, then present our results investigating both the impact of landmark deployment and quantity using our previously defined metrics.

A. Simulation Methodology

Our simulation methodology requires we generate a simulated RSS reading for any point on the floor of a building from any landmark. We first begin with the path loss equation that models the received power as a function of the distance to the landmark:

$$P(d)[dBm] = P(d_0)[dBm] - 10nlog(\frac{d}{d_0}) \quad (14)$$

We choose the parameters $d_0 = 1m$, $P(d_0) = 58.48$ and $n = 1.523$ from [9]. We then apply a random noise factor to perturb the RSS readings. This corresponds to the random model described in [18], which represents an upper bound on the signal variability.

In many cases, we found that the localization error is large enough such that the estimated position is well outside the floor. This was particularly true for LLS. Because such results are unrealistic in our scenario, we apply a simple truncation rule in these cases: if the X or Y coordinate is outside the floor, we truncate to the maximum or minimum value along that dimension.

B. Evaluation of Estimation Error

Table I presents the average location estimation error after the application of truncation and the Hölder metrics for both LS algorithms under 5 landmarks for our two simulated floors. The optimized landmark deployment setup is obtained from the $maxL-minE$ algorithm. It is encouraging that both NLS and LLS provide smallest estimation errors using our placement algorithm. By comparing the values of the Hölder parameters, the LS algorithm is the least susceptible to random noise with the optimized landmark deployment, which has 4 landmarks positioned as the vertex of a square plus the fifth landmark placed at the center of the mass.

When under the diagonal landmark deployment, the localization results suffer the largest estimation errors and the algorithm is the most susceptible. The following results presented in this section are bounded by the floor boundary.

C. Impact of Landmark Deployment

In this section we describe the impact of 3 different deployments on localization performance. We use a representative situation of 5 landmarks deployed in 3 ways to demonstrate the impact of our algorithm in a typical case.

The first deployment we call $square$, and in the 5 landmark case it is an optimal deployment when the shape is a square plus one landmark at the center

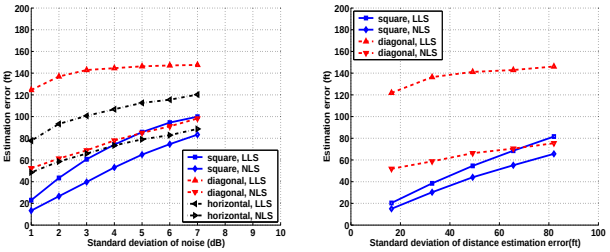

(a) (b)

Fig. 3. In 200x200ft area: (a) Location estimation error vs. random noise in RSS (b) Location estimation error vs. ranging error

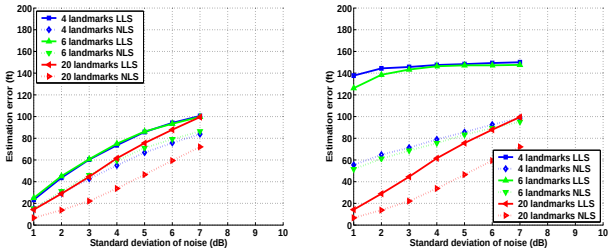

(a)Optimized case (b)Worst case

Fig. 4. Performance of LS algorithms across different number of landmarks in 200x200ft area

deployment	optimal	horizontal	vertical	diagonal
Topology 200x200ft				
Linear LS				
$error$	59.81	101.26	101.07	141.79
H	58.05	172.23	159.01	206.24
$\overline{H}$	8.03	9.51	9.74	9.84
Nonlinear LS				
$error$	39.48	66.82	66.08	70.27
H	75.44	132.61	180.27	230.52
$\overline{H}$	6.98	7.31	7.58	7.97
Topology 230ftx150ft				
Linear LS				
$error$	57.89	86.97	116.57	146.65
H	66.39	170.98	198.44	352.96
$\overline{H}$	7.22	8.20	9.84	8.86
Nonlinear LS				
$error$	39.00	56.24	74.06	61.19
H	80.69	232.88	267.32	265.68
$\overline{H}$	6.66	7.12	7.21	7.32

TABLE I

LOCALIZATION ERROR (FT) AND HÖLDER METRICS WHEN STANDARD DEVIATION OF NOISE ON RSS IS 3DB

of the mass. Next, the $horizontal$ deployment is the one where all the landmarks placed in a line along the longest dimension; this will give better signal coverage than the square for rectangular buildings. Finally, we also examine the impact of a poor deployment, in this case $diagonal$, which equally spaces the landmarks along a diagonal line.

Figure 3(a) shows the average accuracy of 10000 random trials across the floor for the 3 deployments as a function of increasing the standard deviation σ_{rss} of the noise term applied to each point. The six curves correspond to the NLS and LLS for each deployment.

First, NLS always significantly outperforms LLS. When the σ_{rss} is less than 4dB, which is typical based on our experimental experience, both algorithms under the optimized landmark deployment outperform the two other deployments. When the σ_{rss} is larger than 4dB, under the optimized landmark deployment, the NLS still performs better, while the performance of the LLS is compatible with the performance of the NLS for horizontal and diagonal landmark deployments.

Constant sized deviations in the RSS readings result in wide differences in the distance estimation depending on the distance to the landmark. Note that the relationship between the RSS error and ranging error is multiplicative with distance, i.e., $\tilde{d} = d10^{\frac{ss-\hat{ss}}{10n}}$. For example, in our simulation a 3dB error corresponds to a multiplicative factor of 1.5, at 10ft distance, $\tilde{d} = 15ft$ with an error of 5ft, while at 100ft distance, $\tilde{d} = 150ft$ with an error of 50ft, a factor of ten larger. We are motivated to study the magnitude of distance estimation error caused by the deviation of the RSS readings.

Figure 3(b) shows the location estimation error vs. the standard deviation σ_d of distance estimation error. We observe that a noise σ_{rss} of 2dB corresponds to a distance error σ_d of 32ft. Further, the estimation results when the σ_{rss} is 4dB and 5dB translate to the σ_d of 65ft and 82ft respectively. Thus, even small random perturbation in RSS readings cause large ranging estimation errors due to this multiplicative factor.

D. Impact of Landmark Quantity

In this section we observe the impact of adding more landmarks. We compare the performance of the LS algorithms with 4, 6 and 20 landmarks under square and diagonal deployments. We use our optimized placement in the case of 4 and 6 landmarks, and a uniform randomized deployment for 20 landmarks.

Figure 4 shows a promising result that when deploying 4 landmarks and 6 landmarks under their optimized deployments, the localization results using LS are compatible with the results using a much higher number landmarks, 20, in this case. If a small number of landmarks provide sufficient coverage, this is an encouraging observation because good localization performance can be achieved without a large number of landmarks.

VI. EXPERIMENTAL STUDY

In this section we present our experimental study by using 802.11 PCMCIA cards and Telos Sky motes. The objective is to compare the impact of

our landmark deployment analysis on a variety of algorithms and different ranging modalities. Although the mathematics of our analysis is based on LLS, we show that deployments based on $maxL - minE$ algorithm improve localization accuracy in widely diverse scenarios.

We first give a brief description of a set of representative RSS-based localization algorithms. We then describe our experimental method. Next, we quantify the performance across the algorithms provided different landmark deployments. We also compare the localization accuracy and Hölder metrics for these algorithms. Finally, we provide a comparison between the RSS-based and TOA-based LS algorithms using our deployment strategy.

A. Algorithms

In this study, our main focus is the localization algorithms that employ signal strength measurements. To demonstrate the general applicability of our landmark deployment algorithm, we test our placement strategy on three widely different localization algorithms, RADAR, ABP, and BN. Although there are many other RSS-based localization algorithms, this set spans various strategies, and given all algorithms have qualitatively similar performance [10] we feel this set is sufficiently representative.

RADAR is a point-based, scene-matching algorithm. The user first builds a training set of RSS values from landmarks matched to known locations. To localize, the object creates a vector of RSS values from the landmarks and the algorithm returns the training point closest to the vector using Euclidean distance as the discriminating function [9]. ABP uses Bayes rule combined with scene-matching to return an area the object is likely to reside in and probabilistically bounds the likelihood with a confidence level [10]. Taking the Bayesian network approach, the BN algorithm uses a Bayesian graphical model based on lateration to find the estimated location [19].

B. Experimental Setup and Methodology

A series of experiments are conducted in our Computer Science Department which resides the whole 3rd floor of the CoRE building. The floor size is 200x80ft (16000 ft^2). The experiments are performed using 4 landmarks setup in the floor.

Figure 5(a) shows the original collinear landmark deployment setup in triangles and our optimized landmark deployment as squares for the 802.11 network. The networking staff of the department deployed the APs in the collinear deployment specifically to maximize signal strength coverage. The first set of RSS data was collected under this collinear deployment by using a Dell laptop running Linux equipped with an Orinoco silver card (802.11 card). The data was collected at 286 locations on the 3rd floor.

Then we used a trace-driven approach to generate the RSS data set under the optimized landmark deployment. We first performed a least squares fit of the measured data and obtained the parameters of the path loss model in Equation (14). Then we directly used measured variance to generate the RSS readings. Finally, we applied environmental bias using the Ray-Sector model described in [18] to obtain the new RSS data set for the optimized deployment case.

To validate that our trace-driven strategy generated realistic radio signal readings, we placed 4 simulated landmarks at the same positions as the real collinear deployment and then generated synthetic RSS values. We compared the localization performance of using this synthetic data set against the real data. We found the estimation CDFs nearly identical for all of our algorithms under study. Thus we have confidence that our combination of path-loss model fitting, variance application, and bias generation result in RSS readings that generate realistic localization results.

Our second experimental setup was an 802.15.4 network which utilized 4 Telos Sky mote landmarks and deployed two sets of landmark placement positions. Figure 5 (b) shows the mote landmarks under an optimized square deployment as squares and a horizontal landmark deployment (again, to maximize signal strength coverage) as triangles. Unlike the 802.11 case, no RSS data was generated; for both deployments the measured data is used in the algorithms.

We have experimented with different training set sizes for constructing the radio map for RADAR and ABP. For 802.11 data sets, we show the results with 115 training points. While for 802.15.4 data sets, we use 70 training points. The small stars in Figure 5 are the randomly selected training points. The localization at each testing point is performed by using the leave-one-out method.

C. Localization Accuracy

Figure 6 (a) and (b) present the 802.11 accuracy CDF under collinear and square landmark deployments, respectively. A bounded result means we applied truncation. ABP is calculated with confidence level 75%. ABP-med is the error of the median distance of the area, together with ABP-min and ABP-max are the closest and furthest points of the returned area.

Figure 6(a) shows that under the horizontal-like deployment, LLS always fairs very poorly, while NLS,

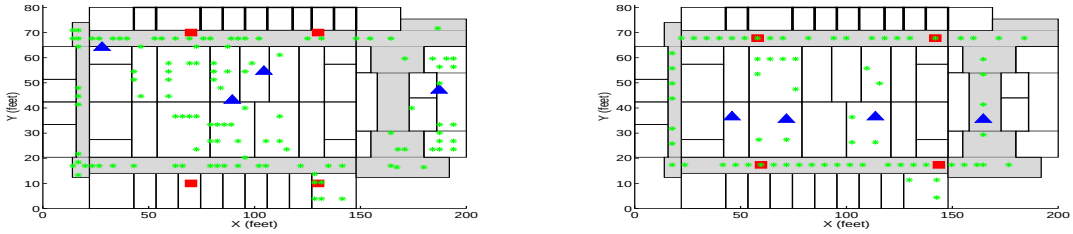

(a)802.11 (b)802.15.4

Fig. 5. Deployment of landmarks and training locations on the experimental floors

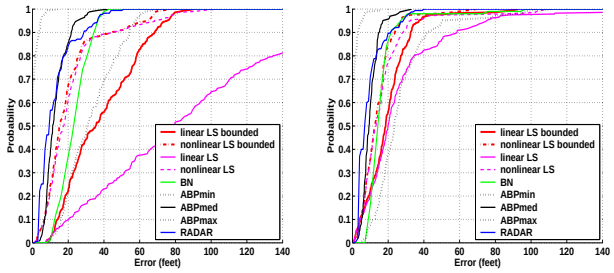

(a)Collinear case (b)Square case

Fig. 6. Localization accuracy CDFs across algorithms for 802.11 network

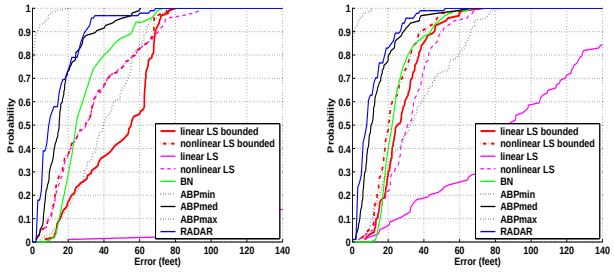

(a)Horizontal case (b)Square case

Fig. 7. Localization accuracy CDFs across algorithms for 802.15.4 network

RADAR, ABP and BN are qualitatively similar. All the algorithms have long tails. Figure 7(a) shows a similar result when using the motes, although in here the perfect collinear deployment, the horizontal case, reduces the performance of the lateration approaches (BN, NLS , and LLS) compared to 802.11.

Figures 6(b) and 7(b) show the key impact of our work. All of the CDFs have shifted up and to the left compared to those in Figures 6(a) and 7(a). Thus, a significant fraction of the results are more accurate using the optimized deployments generated by $maxL - minE$ algorithm. In addition, for ABP, the gap between the min and max CDFs is much narrower, implying the returned areas are on average smaller than those in the horizontal deployments.

D. Evaluation of Performance and Sensitivity

Table II summarizes the average error for each algorithm to further investigate the improvements gained by using an optimal deployment. The table shows the average error improves for all the algorithms. For 802.11 data sets, the LLS algorithm improves over 35% and NLS gains 25% in performance. Both ABP and RADAR have improved over 20% in localization accuracy, while BN has gained 10%. Looking at the 802.15.4 network, the performance improvement results are compatible to the results from the 802.11 network.

The Hölder metrics presented in Table II for each algorithm under the optimized landmark deployment is smaller than the horizontal deployment. Recall that the Hölder parameter is a measurement of the sensitivity of the algorithm to perturbations of inputs such as RSS, which can model random noise, environmental bias, and measurement errors. The lower Hölder values are strong evidence that an optimized landmark deployment not only can improve the localization performance, but also can make an algorithm less susceptible to the above classes of perturbations.

E. Using Time of Arrival

In this section we experimentally investigate how well our deployment algorithm works for an alternate ranging modality. In this second modality, we compute the distance to a landmark by measuring many round trip times between a node and a landmark, and then calculate the time-of-flight (ToF) of a packet. Given the ToF and the speed of light, we can estimate the range. This is a Time-of-Arrival (TOA) based approach because the actual time-of-flight is estimated. Space limitations prevent us from describing this approach in more details, but a full description of the technique and an analysis of it can be found in [20].

We used a similar trace-driven based methodology in our TOA investigation as for the 802.11 RSS one. We estimated the TOA based on the round trip times for packets and derived the distance between the localizing node to each landmark. We then built an error distribution of the true distance vs. the estimated distance, and used that to drive a simulation where we could place the landmarks in the same positions as the RSS study. The same hardware is used as for

average location estimation error							
Algorithms	**Linear LS**		**Nonlinear LS**		**BN**	**ABP**	**RADAR**
802.11	**w trun**	**w/o trun**	**w trun**	**w/o trun**			
collinear	38.56	94.53	20.23	21.85	22.25	13.11	12.49
square	24.73	31.29	15.37	16.92	20.16	10.09	9.31
802.15.4	**w trun**	**w/o trun**	**w trun**	**w/o trun**			
horizontal	47.89	608.43	33.15	34.44	28.43	17.86	14.28
square	28.27	92.05	23.65	32.17	24.25	14.27	11.33
Hölder	**(worst-case)** H						
Algorithms	**Linear LS**		**Nonlinear LS**		**BN**	**ABP**	**RADAR**
802.11	**w trun**	**w/o trun**	**w trun**	**w/o trun**			
collinear	22.36	48.47	21.55	21.55	31.73	20.03	36.24
square	12.19	15.33	9.62	9.75	15.89	10.64	9.86
802.15.4	**w trun**	**w/o trun**	**w trun**	**w/o trun**			
horizontal	28.88	286.13	91.00	91.00	28.27	64.06	32.58
square	13.86	17.14	10.82	16.32	18.41	11.27	13.42
Hölder	**(average-case)** $\overline{H}$						
Algorithms	**Linear LS**		**Nonlinear LS**		**BN**	**ABP**	**RADAR**
802.11	**w trun**	**w/o trun**	**w trun**	**w/o trun**			
collinear	2.72	5.37	2.06	2.18	2.06	1.85	1.98
square	2.87	3.57	2.45	2.70	1.63	1.79	2.06
802.15.4	**w trun**	**w/o trun**	**w trun**	**w/o trun**			
horizontal	2.66	33.87	2.45	2.50	1.44	2.05	2.21
square	2.95	5.23	2.35	2.69	2.41	1.95	2.27

TABLE II

LOCATION ESTIMATION ERROR (FT) AND HÖLDER PARAMETERS ACROSS ALGORITHMS

the RSS study.

The linear regression model applied to the distance estimation error of TOA data with 63 experimental distances is shown in Figure 8(a). We observe that shorter the distance to a landmark results in estimated distance longer than the true distance, while longer the distance to a landmark results in estimation distance shorter than the true distance. The corresponding distance estimation error of RSS data is presented in Figure 8(b). Comparing the TOA results to RSS distance estimation errors, while the magnitude of the distance estimation error grows with lengthening distance, unlike in TOA the resulted estimation in RSS is longer or shorter with near equal probability.

With the mean and variance estimated from linear regression, we have modeled distance estimation error of TOA as a Gaussian distribution defined in Equation (15):

$$\begin{aligned} error &\sim N(\mu, \sigma^2) \\ with\ \hat{\mu} &= b_0 + b_1 d_i \\ and\ \hat{\sigma^2} &= \frac{\sum_{i=1}^{n} (\tilde{d_i} - \hat{\mu})^2}{n-1}, \end{aligned} \tag{15}$$

where d_i is the true distance and $\tilde{d_i}$ is the estimated distance. n is the total number of distances under experimentation. b_0 and b_1 are the coefficients of the linear regression.

We further conducted a trace-driven approach to localize 286 positions on the floor using 4 landmarks setup with collinear and square deployment respectively according to Figure 5(a) for the 802.11 network.

Figure 9 plots the localization accuracy CDF of the

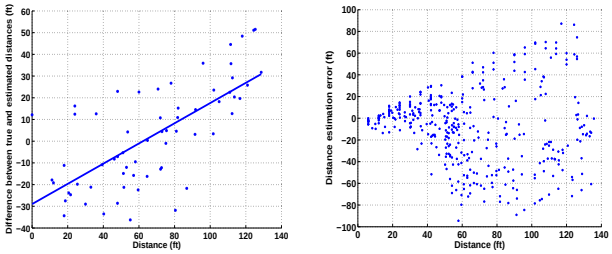

(a)TOA (b)RSS

Fig. 8. Linear regression on TOA data

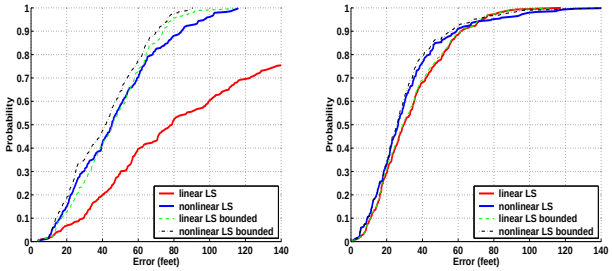

(a)Collinear case (b)Square case

Fig. 9. Localization accuracy CDFs using TOA

LS algorithms using TOA. The figure shows that as with RSS, the performance of LS increases under an optimized deployment as compared to a horizontal deployment designed for coverage. Quantitatively, the performance improvement is over 30%. Comparing the absolute performance of this technique with RSS, our TOA approach is qualitatively worse. This is likely due to the very coarse grained microseconds-level clocks currently available in standard 802.11. Additional clocks with much higher frequencies would help to reduce much of the measurement uncertainty.

VII. Conclusion

By analyzing the Linear Least Squares algorithm, we derived an upper bound on the maximum location error given the placement of landmarks. Based on this theoretical analysis, we found optimal patterns for landmark placement and further developed a novel algorithm, $maxL - minE$, for finding optimal landmark placement that minimizes the maximum localization error.

To show the generality of our results, we conducted experiments using both an 802.11 (WiFi) network and an 802.15.4 (ZigBee) network. Based on the experimental data, we investigated the impact of landmark position and quantity on localization performance using both the measurements of RSS in an actual building as well as trace-driven simulations that used the RSS measurements. In addition, we apply the trace-driven approach to an alternate ranging modality, in this case, TOA.

We found that the performance of a wide variety of algorithms showed significant improvements when using landmarks placed according to our algorithm, as opposed to alternate deployments. We evaluated these improvements under several different metrics. The experimental results provide strong evidence that our analysis and algorithm for landmark placement is very generic as the resulting placement has improved localization performance across a diverse set of algorithms, networks, and ranging modalities.

Our results also point out that there is a tension between the ideal landmark deployment for localization vs. deployments that optimize for signal coverage. We found that in our building, the better coverage deployment was very collinear, and this had pronounced negative impact on localization performance. Future work would conversely investigate the impact of a deployment optimized for localization on signal coverage, as well as try to find a method of trading one kind of deployment for another depending on the users' needs.

References

[1] P. Enge and P. Misra , *Global Positioning System: Signals, Measurements and Performance*. Ganga-Jamuna Pr, 2001.

[2] D. Niculescu and B. Nath, "Ad hoc positioning system (APS)," in *Proceedings of the IEEE Global Telecommunications Conference (GLOBECOM)*, 2001, pp. 2926–2931.

[3] K. Langendoen and N. Reijers, "Distributed localization in wireless sensor networks: a quantitative comparison," *Comput. Networks*, vol. 43, no. 4, pp. 499–518, 2003.

[4] Z. Li, W. Trappe, Y. Zhang, and B. Nath, "Robust statistical methods for securing wireless localization in sensor networks," in *Proceedings of the Fourth International Symposium on Information Processing in Sensor Networks (IPSN)*, 2005.

[5] K. Chintalapudi, A. Dhariwal, R. Govindan, and G. Sukhatme, "Ad hoc localiztion using ranging and sectoring," in *Proceedings of the IEEE International Conference on Computer Communications (INFOCOM)*, March 2004.

[6] R. Battiti, M. Brunato, and A. Delai, "Optimal wireless access point placement for location-dependent services," Department of Information and Communication Technology, University of Trento, Italy, Technical Report DIT-03-052, October 2003.

[7] Y. Chen, K. Kleisouris, X. Li, W. Trappe, and R. P. Martin, "The robustness of localization algorithms to signal strength attacks: a comparative study," in *To appear in Proceedings of the International Conference on Distributed Computing in Sensor Systems (DCOSS)*, June 2006.

[8] N. Patwari, J. N. Ash, S. Kyperountas, A. O. Hero, R. L. Moses, and N. S. Correal, "Locating the nodes," *IEEE Signal Processing Magazine*, July 2005.

[9] P. Bahl and V. N. Padmanabhan, "Radar: An in-building rf-based user location and tracking system," in *Proceedings of the IEEE International Conference on Computer Communications (INFOCOM)*, March 2000.

[10] E. Elnahrawy, X. Li, and R. P. Martin, "The limits of localization using signal strength: A comparative study," in *Proceedings of the First IEEE International Conference on Sensor and Ad hoc Communcations and Networks (SECON 2004)*, Oct. 2004.

[11] N. Priyantha, A. Chakraborty, and H. Balakrishnan, "The cricket location-support system," in *Proceedings of the ACM International Conference on Mobile Computing and Networking (MobiCom)*, Aug 2000.

[12] Y. Shang, W. Ruml, Y. Zhang, and M. P. J. Fromherz, "Localization from mere connectivity," in *Proceedings of the Fourth ACM International Symposium on Mobile Ad-Hoc Networking and Computing (MobiHoc)*, Jun 2003.

[13] M. Youssef, A. Agrawal, and A. U. Shankar, "WLAN location determination via clustering and probability distributions," in *Proceedings of IEEE PerCom'03*, Fort Worth, TX, Mar. 2003.

[14] T. Roos, P. Myllymaki, and H.Tirri, "A Statistical Modeling Approach to Location Estimation," *IEEE Transactions on Mobile Computing*, vol. 1, no. 1, Jan-March 2002.

[15] L. Doherty1, K. S. J. Pister, and L. ElGhaoui, "Convex position estimation in wireless sensor networks," in *Proceedings of the IEEE International Conference on Computer Communications (INFOCOM)*, Apr. 2001.

[16] Y. Chen and H. Kobayashi, "Signal strength based indoor geolocation," in *Proceedings of the IEEE International Conference on Communications (ICC)*, April 2002.

[17] A. Krishnakumar and P. Krishnan, "On the accuracy of signal strength-based location estimation techniques," in *Proceedings of the IEEE International Conference on Computer Communications (INFOCOM)*, March 2005.

[18] X. Li and R. Martin, "A simple ray-sector signal strength model for indoor 802.11 networks," in *Proceedings of the Second IEEE International Conference on Mobile Ad-hoc and Sensor Systems (MASS)*, November 2005.

[19] D. Madigan, E. Elnahrawy, R. Martin, W. Ju, P. Krishnan, and A. S. Krishnakumar, "Bayesian indoor positioning systems," in *Proceedings of the IEEE International Conference on Computer Communications (INFOCOM)*, March 2005, pp. 324–331.

[20] A. Gunther and C. Hoene, "Measuring round trip times to determine the distance between WLAN nodes," Technical University Berlin, Telecommunication Networks Group, Technical Report TKN-04-16, December 2004.